Tandem Adjoint Level Set Topology and Shape Optimization for 2D and 3D Internal Flows

James R. L. Koch*, Evangelos M. Papoutsis-Kiachagias, Kyriakos C. Giannakoglou
National Technical University of Athens (NTUA)
School of Mechanical Engineering, Parallel CFD & Optimization Unit Athens, Greece
Email: kochjamesr@gmail.com, vaggelisp@gmail.com, kgianna@central.ntua.gr

Summary

Topology and shape are two of the main classifications of optimization in the field of fluid mechanics and are generally treated as mutually exclusive, with topology defining a geometric solution when only the inlets and outlets of a flow problem are known and shape finding a physically accurate optimal shape for a known initial flow geometry. This paper (being sequel to a previous publication exclusively on 2D problems) presents the TtoST transitional process to allow the continuous-adjoint-driven optimization of these two methods to be employed in tandem by representing (2D and) 3D topology solutions with NURBS-parameterization from which shape optimization be initialized. By utilizing the level set method, a convenient representation of the interface between the solid and fluid topological domains is maintained throughout the topology process. The interface is fit with non-uniform rational B-spline (NURBS) curves (2D) or surfaces (3D) by solving an auxiliary inverse design problem which aims at reducing the difference between signed-distance fields generated about both the NURBS curves or surfaces being optimized and the section of interface being fit. A shape optimization loop is then run on a body-fitted grid generated from the geometry defined by the fitted NURBS parameterization. In the full paper, results of the tandem topology-shape process will be presented for both 2D and 3D internal, incompressible fluid flow cases.

Keywords: *Topology-to-Shape Transition, CAD-compatibility, Constrained Topology Optimization, Level Set Method, Shape Optimization, Adjoint-Based Optimization*

Introduction

In the field of fluid mechanics, topology optimization (TopO) introduces a 'blockage' term (β) into the flow equations[1,3] which acts as a design variable for each grid cell and is controlled to minimize an objective function. In contrast, shape optimization (ShpO) reduces an objective function[4] by altering the original boundary shape constraining the flow solution. In this paper, both techniques employ the continuous adjoint method[5,6] to drive design variables of a given problem toward an optimal value-set such that the objective function(s) are minimized or maximized.

This paper considers the benefits in conjoining the TopO and ShpO processes, i.e. taking a TopO solution and using it to initialize a ShpO process via the Topology to Shape Transition (TtoST) process which has been developed in 2D[11,12] and is expanded upon in 3D in this work. To properly initialize a ShpO solution, information pertaining to TopO's internal-flow boundaries (the 'interface' between fluid and solid domains) is required. In this work, such information is defined using the level set (LS) approach and specifically its zero contour. First proposed in,[7] the LS method is a conceptual framework which introduces a signed-distance LS field through which moving interfaces can be mapped. To integrate the LS method into TopO, β is replaced by a function of the LS field, ϕ. To progress the interface toward the optimal solution, the cell-centered LS field is updated utilizing adjoint-based sensitivities and corrected through application of an accurate, fast-marching signed-distance correction algorithm.

In 2D problems, the TopO-to-ShpO transition process subdivides the TopO solution's interface into segments which pertain to the connections between the inlets and outlets. These interface segments are used to construct individual signed-distance fields which act as target solutions to an inverse design problem (referred to as the 'field matching' problem) which tries to iteratively fit a non-uniform rational B-spline (NURBS) curve to each segment. The NURBS curve's control points are computed by minimizing the difference between a narrow band (NB) signed-distance field built about each NURBS curve and that curve's target signed-distance field. A body-fitted grid is then generated from the fitted NURBS curve and used to initialize an adjoint-driven ShpO process, resulting in a parameterized optimal solution.

In 3D, sub-division of the TopO solution's interface becomes more complicated. The interface is divided into patches to be represented by individual NURBS surfaces, such that interface connections between inlets and outlets are represented by non-overlapping, air-tight sets of such patches. Each connection's patch set is used to construct the target signed-distance field for the field-matching inverse design problem, the solution process of which is similar to that of the 2D problem, with the notable difference that the simultaneous (and contiguous) movement of all NURBS surfaces pertaining to the patches in the connection-set is now required. Once all sets of NURBS surfaces are fit, a boundary-fitted grid is generated to initialize an adjoint-driven ShpO process.

This paper exemplifies the proposed method for conjoining the TopO and ShpO processes through: *a*) a 2D internal-flow three-manifold case in which the volume-averaged total pressure losses between the inlet(s) and outlet(s) is desired to be reduced while retaining equal mass flow between each of the manifold's outlets, *b*) a 3D internal-flow straight channel case. All cases and in-house code pertaining to the coupling process are implemented within OpenFOAM 2.2.1.[8]

Topology Optimization

Flow Equations

The flow modeled in this paper is governed by the steady-state Navier-Stokes equations for laminar, incompressible fluids for which the bulk viscosity ν is fixed. As with all equations found in this Section, repeated indices indicate Einstein summation.

$$R_p = -\frac{\partial v_j}{\partial x_j} = 0 \tag{1a}$$

$$R_{v_i} = v_j\frac{\partial v_i}{\partial x_j} + \frac{\partial p}{\partial x_i} - \frac{\partial}{\partial x_j}\left[\nu\left(\frac{\partial v_i}{\partial x_j}+\frac{\partial v_j}{\partial x_i}\right)\right] + H(\phi)\beta_{MAX}v_i = 0 \tag{1b}$$

In the LS blockage formulation of TopO, the addition into the momentum equation which constrains the velocity with a Heaviside $H()$ of the level set variable ϕ (see eq. (9)) scaled with the large, positive user-defined value β_{MAX}. If $H(\phi)$ approaches 1, the added term becomes dominant, forcing the velocity toward zero and effectively obstructing flow. Conversely, if $H(\phi)$ approaches 0, the flow is uninhibited.[1,2] Section 2.4 presents the LS formulation. The usual boundary conditions (prescribed inlet velocity, constant outlet pressure and no-slip condition along the walls) are imposed.

Objective and Constraint

The objective function J to be minimized is that of the volume-averaged total pressure losses between the inlet(s), S_I, and outlet(s), S_O,

$$J = -\int_{S_I}\left(p+\frac{1}{2}v_k^2\right)v_i n_i dS - \int_{S_O}\left(p+\frac{1}{2}v_k^2\right)v_i n_i dS \tag{2}$$

where n_i are the components of the outward (from the fluid to boundary) normal vector.

To account for the possible inclusion of an equality constraint $C = 0$ into the TopO process, J is re-defined as the Lagrangian function L according to the Augmented Lagrange Multiplier (ALM) method.[9] In this work, the constraint prescribes percentages of exiting volume flow rate to outlets. Written along the O outlets, this volume flow rate constraint function is defined as

$$C = \frac{1}{2}\sum_{o=1}^{O}\left(\int_{S_{O_o}} v_i n_i dS + r_o\int_{S_{I_{ALL}}} v_i n_i dS\right)^2 = 0 \tag{3}$$

where $0 \le r_o \le 1$ is the desired volume flow rate ratio from the o^{th} outlet expressed as a percentage of the incoming flow rate, with $\sum_{o=1}^{O} r_o = 1$.

Adjoint Equations, Boundary Conditions and Sensitivities

To formulate the adjoint field equations and boundary conditions, the Lagrangian is further augmented by the flow equation residuals as follows

$$L_{aug} = L + \int_\Omega q R_p d\Omega + \int_\Omega u_i R_{v_i} d\Omega \tag{4}$$

with q and u_i being the adjoint pressure and adjoint velocity components, respectively. After lengthy derivation,[10] the variation of eq. (4) w.r.t. the level set design variable set ϕ becomes

$$\begin{aligned}\frac{\delta L_{aug}}{\delta\phi_m} = &\int_\Omega R_q\frac{\partial p}{\partial\phi_m}d\Omega + \int_\Omega R_{u_i}\frac{\partial v_i}{\partial\phi_m}d\Omega \\ &+ \int_\Omega v_i u_i\frac{\partial H(\phi_m)\beta_{MAX}}{\partial\phi_m}d\Omega \\ &+ \int_S \mathscr{BC}_1\frac{\partial p}{\partial\phi_m}dS + \int_S \mathscr{BC}_{2,i}\frac{\partial v_i}{\partial\phi_m}dS \\ &- \int_S\frac{\partial}{\partial\phi_m}\left[\nu\left(\frac{\partial v_i}{\partial x_j}+\frac{\partial v_j}{\partial x_i}\right)\right]u_i n_j dS\end{aligned} \tag{5}$$

where m is the computational cell index and S is the boundary of the computational domain Ω. For simplicity, L_{aug} will be referred to as L for the remained of this work. The R_q and R_{u_i} terms in eq. (5) become the adjoint field equations by eliminating all terms with field integrals containing derivative(s) of the flow variables w.r.t. the design variables by setting their multipliers against zero.

The adjoint continuity and momentum field equations which make $\frac{\delta L}{\delta\phi_m}$ independent of $\frac{\partial p}{\partial\phi_m}$ and $\frac{\partial v_i}{\partial\phi_m}$ are

$$R_q = \frac{\partial u_j}{\partial x_j} = 0 \tag{6a}$$

$$R_{u_i} = -v_j\left(\frac{\partial u_i}{\partial x_j}+\frac{\partial u_j}{\partial x_i}\right) + \frac{\partial q}{\partial x_i} - \frac{\partial}{\partial x_j}\left[\nu\left(\frac{\partial u_i}{\partial x_j}+\frac{\partial u_j}{\partial x_i}\right)\right] + H(\phi)\beta_{MAX}u_i = 0. \tag{6b}$$

The $\mathscr{BC}$ terms in eq. (5) are related to the adjoint boundary conditions in that they describe conditions to be met in order

for $\frac{\delta L}{\delta \phi_m}$ to become independent of partial derivative(s) of the flow variables w.r.t. the design variable set along the boundary.[10] After satisfaction of the field adjoint equations and their boundary conditions, eq. (5) defines the sensitivity derivatives of L w.r.t. the blockage field design variables,

$$\frac{\delta L}{\delta \phi_m} = \int_\Omega v_i u_i \frac{\partial H(\phi_m)\beta_{MAX}}{\partial \phi_m} d\Omega = \beta_{MAX} D(\phi_m) v_i^m u_i^m \Omega^m \tag{7}$$

where the scaled LS Heaviside function $H(\phi)$ and its derivative $D(\phi)$ depend only on the m-th grid cell with volume Ω^m associated with the discrete description of the field domain.

Level Set Topology Formulation

To conveniently describe TopO's interface throughout its optimization process, the LS method was employed to control flow blockage and will hereafter be synonymous with the term TopO. The LS method represents design domains in terms of a signed-distance function ϕ which is differentiable at the interface Γ separating them, and must have a gradient magnitude of 1 everywhere ($\|\nabla\phi\| = 1$) such that $\phi_i = \{\text{negative } \forall\ i \in \Omega_{\text{Solid}},\ \text{zero } \forall\ i \in \Gamma,\ \text{positive } \forall\ i \in \Omega_{\text{Fluid}}\}$.

The LS field can be initialized from any existing blockage field $0 \leq \beta \leq 1$ through the relation

$$\phi_m = \phi(\beta_m) = 1 - 2\beta_m \tag{8}$$

which defines a starting Γ. The LS contribution to the blockage terms of the flow equations is the continuously differentiable, piecewise NB sigmoidal Heaviside relationship

$$H(\phi_m) = \begin{cases} 1 & \phi_m < -d_{NB} \\ \frac{1}{2}\left[1 - \frac{\phi_m}{d_{NB}} - \frac{1}{\pi} sin\left(\frac{\pi\phi_m}{d_{NB}}\right)\right] & |\phi_m| \leq +d_{NB} \\ 0 & \phi_m > +d_{NB} \end{cases} \tag{9}$$

where $d_{NB} > 0$ is the user-defined normal distance from Γ (in either direction) which sets the limits of the NB. To ensure stable convection, d_{NB} is limited to include a single cell on either side of Γ. This Heaviside function differentiates into a finite and continuous function $D(\phi_m)$, *i.e.*,

$$\frac{\delta H(\phi_n)}{\delta \phi_m} = D(\phi_m)\delta_m^n \tag{10}$$

where δ_m^n is a Kronecker delta.

To move Γ toward the optimal solution, the LS field is subjected to a process of convection by solving what is practically a steepest-descent step for the ϕ field

$$\frac{\partial \phi_m}{\partial t} + V_m = 0 \tag{11}$$

where V_m is provided by eq. (7) and $\|\nabla\phi\| = 1$ should hold. After eq. 11 is explicitly applied to Γ, $\|\nabla\phi\| = 1$ does not necessarily hold, requiring that the ϕ field undergo a signed-distance correction procedure after each convection application. The procedure employed in this paper efficiently corrects ϕ_m within the cells holding Γ using the existing ϕ values of those cells and then conducts a fast marching method to correct the remainder of the NB.[13]

To summarize the LS-TopO process, which is identical in 2D and 3D, ϕ is initialized from an existing β field via eq. (8), and then the following process is repeated until the optimal solution is obtained. First, eqs. (1), followed by eqs. (6) are solved iteratively to get the the flow and adjoint solutions, respectively. Next, $D(\phi_m)$ and the LS convecting scalar velocities V_n are computed via eqs. (10) and (11), and are used to progress Γ toward the optimal solution by updating ϕ. The correction process is conducted to get correct ϕ values within the NB of the newly convected Γ.

Topology-to-Shape Transition (TtoST)

The process of ShpO implemented in this work takes parameterized (CAD-compatible) curves or surface as inputs in order to build a computational grid from which to start. In the present work, these inputs are comprised of NURBS. In order to allow a tandem TopO-ShpO optimization to occur, a transitional method has been developed in 2D[12] and is here extended to 3D to automatically generate and fit, as closely and efficiently as possible, NURBS to TopO solutions so as to have an initial boundary which matches the TopO geometry and can be fed directly into a meshing program to begin the ShpO process.

The procedure for the proposed TopO-to-ShpO process (TtoST) is divided into four main steps: Γ segmentation, NURBS initialization, 'target' signed-distance field generation and fit refinement via a 'field matching' algorithm,[12] and can vary significantly between 2D and 3D geometries. Results for application of the TtoST process can be seen in Section 4.1 for 2D and Section 4.2 for 3D. The boundaries of all computational grids are denoted as S, with the subscripts I, O, Y, W and FW designating inlet, outlet, symmetry, 'design' walls (for TopO: walls which can potentially hold Γ; for ShpO: the parameterized walls) and 'fixed' walls (fluidized walls not pertaining to the design space, and which for TopO do not hold Γ and for ShpO are not parameterized), respectively.

2D TtoST in Brief

To initialize ShpO, a grid with parameterized boundaries must be generated. In 2D, such a grid is constructed from a contiguous set of NURBS curves which accurately represent the solution obtained by TopO. Firstly, the TtoST process finds target information to be fit by NURBS curves, dividing the Γ information contained in TopO's ϕ solution into portions (referred to as 'isoSegs') which pertain to each relevant inlet-outlet connection. The TtoST process marches along the faces holding Γ, generating ordered points which are assigned parametric values for initializing NURBS curves via a one-shot least-squares initialization

method. Such curve initialization is done with a pre-defined degree and number of control points (NCPs) for all isoSeg targets.

As this 'naive' fit may be poor, a search for a more desirable degree and number of control points can be optionally conducted by the TtoST process. Then, a 'field matching' design problem is solved for each curve which attempts to minimize the difference between two signed-distance fields: ϕ_{Tar}, generated from the curve's target-portion of Γ, and ϕ_N, generated outward from the NURBS curve up to a defined distance d_{NB} ($0.1m$ for all curves in the manifold case). The generation of these signed-distance fields is conducted using a signed-distance correction process similar to that used in Section 2.4.

Since the field matching process desires to find the optimal location of each NURBS curve's set of control points, its design variables are the degrees of freedom of those control points B_q^n, where q is the control point's index (within the total control point set) and n is the control point's degree of freedom index. The field matching objective and sensitivity derivatives are

$$J_{FM} = \frac{1}{2}\int_\Omega H_2(\phi_N)(\phi_N - \phi_{Tar})^2 d\Omega \tag{12}$$

$$\frac{\delta J_{FM}}{\delta B_q^n} = \int_\Omega \Bigg[\frac{1}{2}\frac{\partial H_2(\phi_N)}{\partial \phi_N}(\phi_N - \phi_{Tar})^2 + H_2(\phi_N)(\phi_N - \phi_{Tar})\Bigg]\frac{\delta \phi_N}{\delta B_q^n} d\Omega \tag{13}$$

with $H_2(\phi_N)$ is a double Heaviside function which allows only the curve's NB to be considered for integration. For the manifold case, the radial extent of this Heaviside is $0.01m$. For a cell m within Ω, the following sensitivity results[12]

$$\frac{\delta \phi_m}{\delta B_q^n} = \frac{p_j^n - c_{m(j)}^n}{\phi_m} N_q(u_j) \tag{14}$$

with p_j being the point on the curve upon which cell m's signed-distance value depends, u_j being the corresponding parametric coordinate, and $N_q(u_j)$ evaluating the NURBS's derivative contribution at that parametric point u_j. The field matching algorithm progresses iteratively as follows until the change in J_{FM} (eq. (12)) falls below a user-defined value. First, ϕ_N is built outward from the curve attempting to fit the isoSeg. Then, sensitivities are found via eq. (13) and the curve's control points are moved. Eq. (12) is evaluated and convergence is checked.

3D TtoST in Brief

In 3D, the parameterized boundaries from which ShpO grids will be constructed are defined by the contiguous set(s) of NURBS surfaces found via the 3D TtoST process. Γ is described by an 'isoMesh' which is constructed from the known connectivity of Γ's interpolated 'isoPts'. The target information to be fit consists of air-tight sub-divisions of this isoMesh referred to as 'isoPatches', which must be constructed such that a single NURBS surface can represent it. The isoMesh is built outward from the edges of 'source' boundary patches types (inlet, outlet and permeable-e.g. symmetry plane). In this way, the important boundary information of the case is retained for ShpO. There are effectively two portions of the isoMesh: source, built along S_I, S_O and S_Y, and internal, built along Γ, S_{DW}, and S_{FW}. To sub-divide the isoMesh into isoPatches, a marching algorithm is performed outward from the source edges which claims faces of the isoMesh by isoPatch ID until another isoPatch's marching front is encountered, forming a set of contact fronts between isoPatches. For each contact front, the isoPatch must generate a splitting connection between it and its source edge.

To define a NURBS surface via skinning, pairs of u and v parametric bases are defined, with each pair having a uniform knot vector of the same size. The target u and v portions of each NURBS surface are found by sorting the isoSegs pertaining to that surface's isoPatch into four ordered sets. To define the uniform knot vectors, the number of control points to represent each isoSeg must be defined. Once the NCPs of each isoSeg, and therefore the uniform knot vectors, have been defined, the NURBS surfaces are generated with a skinning algorithm. Since all NURBS surfaces share a degree, the 3D parameter search only searches for the best-fit degree, in a manner analogous to the 2D parameter search.

Once initialized, the field matching process can be performed on the set of contiguous NURBS surfaces. For each independent set of surfaces pertaining to inlet-outlet connections, a target signed-distance field is generated in the same manner as 2D. Subsequently, the field matching procedure is applied in a two-step process. First, the 'wireframe' of the NURBS set is fit, i.e. the sensitivities found are only applied to the control points shared by one or more NURBS surfaces. Displacement of wireframe control points is fixed if they are shared with a NURBS surface representing S_I or S_O, and restricted to planar motion if shared with a NURBS surface representing S_Y. Then, the control net of all surfaces is fit, i.e. the sensitivities found are only applied to the internal control points of each surface. The objective (and therefore the sensitivities) of the field matching process are trivially extended to 3D, with the only difference being that eq. 14 becomes

$$\frac{\delta \phi_m}{\delta B_q^n} = \frac{p_j^n - c_{m(j)}^n}{\phi_m} N_q(u_j) M_q(v_j) \tag{15}$$

where $N_q(u_j)$ evaluates the NURBS's u-basis' derivative contribution at that parametric point u_j and $M_q(v_j)$ evaluates the NURBS's v-basis' derivative contribution at that parametric point v_j.

Shape Optimization in Brief

Once Γ is accurately and parametrically represented via the TtoST process, a boundary-fitted grid is generated so that ShpO can run. The flow and adjoint equations (and boundary conditions) for the ShpO are identical to eqs. (1)

and (6) if the blockage terms are excluded. The design variables b_l for ShpO are the degrees of freedom of the control points which define its parameterized boundaries. The sensitivities for the ShpO control points are computed via

$$\frac{\delta J}{\delta b_l} = -\int_{S_{DW}} \left[\left(\nu \left(\frac{\partial u_i}{\partial x_j} + \frac{\partial u_j}{\partial x_i} \right) n_j - q n_i \right) \frac{\partial v_i}{\partial x_k} \frac{\delta x_k}{\delta b_l} - (qR_p + u_i R_{v_i}) n_k \frac{\delta x_k}{\delta b_l} \right] dS \quad (16)$$

where $\frac{\delta x_k}{\delta b_l}$ is computed analytically through the NURBS formula.[6]

Tandem Optimization Cases

All geometries presented employ S_{FW} entrance channels to develop boundary layer profiles between the inlets and outlets of a case and that case's design domain (the portion of the case in which β is allowed to be convected). The grids of all cases are Cartesian, with a uniform edge length as stated. The kinematic viscosity ν of all flows presented is $1.5x10^{-5}\frac{m^2}{s}$, and the uniform velocity defined for each case defines a Reynolds number of 500. The objective function J is given by eq. (2). For the LS process, d_{NB} was selected to be equal to the grid's Cartesian edge length. Initially, the internal field is specified as fluid ($\beta = 0$) and all cells owned by the design walls (S_{DW}) are specified as solid, and thus initially hold Γ. For all ShpO cases, S_I, S_O, S_Y and S_{FW} boundaries are considered fixed during the optimization process.

2D Test Case: Triple-Outlet Manifold

The 2D Triple-outlet manifold case consists of an inlet and three outlets of uniform width and spacing. The TopO grid has 33000 cells with edge length $0.001[m]$. The velocity at the inlet is $0.15\frac{m}{s}\hat{x}_1$ ($\hat{x}_i$ is the unit vector along the i^{th} Cartesian axis). The mass fraction constraint was specified to enforce 33% of the inlet flow for all outlets. The geometric data and ϕ field solution (found by the TopO process) of the manifold case are shown in fig. 1. Γ is labeled according to how the TtoST algorithm subdivides it into isoSegs.

The least-squares initialization and field matching fit of the curves representing the manifold case's four TtoST isoSegs can be seen in fig. 2. In order, the final degrees and number of control points the TtoST process found for each curve are 4, 3, 3, 7, and 7, 7, 9, 9, respectively. Although the initialization of the curves is fairly accurate, the field matching algorithm allows all aspects of Γ to be parametrically represented with a high degree of accuracy.

After conducting a ShpO on a boundary fitted grid of 67000 cells, the objective function was reduced by 3.4% and the prescribed mass fraction out of each outlet was maintained. The boundary of ShpO solution is compared to the parameterized TtoST NURBS solution in fig. 3. ShpO process deemed to expand all channels of the manifold,

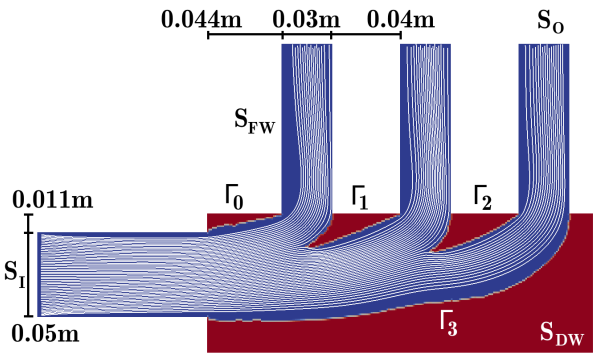

Figure 1: The TopO minimal volume-averaged total pressure loss and mass-fraction constrained ϕ solution and geometry of the 2D manifold case. The solution's Γ exists between between the fluid (red) and solid (blue) level set domains. Portions of Γ pertaining to inlet-outlet connections are labeled according to how the TtoST process defines isoSegs.

compensating for the fact that TopO's Γ does not have boundary conditions imposed upon it.

3D Test Case: Straight Channel

The 3D straight channel case consists of one inlet and outlet of identical size. The grid has 50000 cells with edge length $0.02[m]$. The velocity at the inlet is $0.0375\frac{m}{s}\hat{x}_1$. No mass fraction constraint was specified as only one outlet exists. The geometric data and ϕ field solution (found by the TopO process) of the straight channel case are shown in fig. 4.

The result of the TtoST's sub-division procedure on the straight channel's Γ can be seen in fig. 5. The TtoST algorithm first builds the isoMesh from the source edges of S_I and S_O, first traveling inward on S_I and S_O, then outward across S_{FW} and Γ. Information concerning the segregation of S_{FW} and Γ within the isoMesh is stored. Then, the isoMesh is divided into isoPatches to be fit by NURBS surfaces. S_I and S_O isoPatches are generated first, followed by those representing Γ and S_{FW}. The isoPatch edges are divided into isoSeam point sets which are shared by pairs of isoPatches. These isoSeams are ordered individually for each isoPatch to make portions of its their edges represent targets for the u and v basis of the NURBS surfaces to fit them.

Conclusions

The TtoST method discussed in this work allows for topology optimization and shape optimization to be considered in tandum by representing the interface of topology solutions in a parameterized manner. Specifically, this paper expanded the previously published 2D TtoST process to 3D solutions and showcased the basic 3D steps through a straight channel case. In the full paper, the remaining results for the 3D case (those of NURBS surface

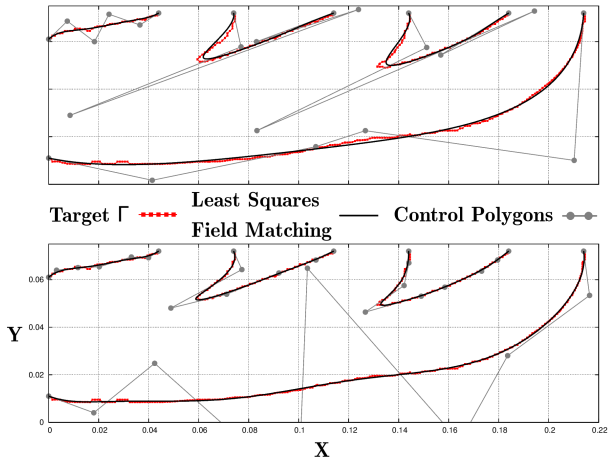

Figure 2: TtoST fitting of the manifold case's isoSegs: (top): the least-squares initialization. (bottom): the result of the field matching process, resulting in an accurate representation of Γ. Both plots include the control polygons of all NURBS curves.

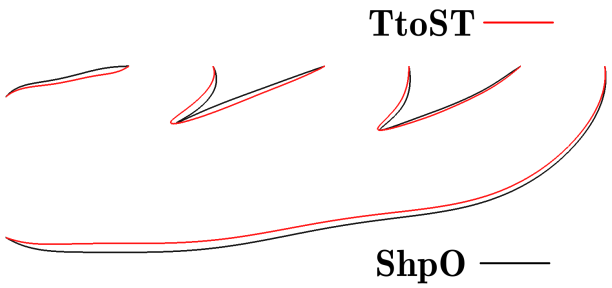

Figure 3: The ShpO solution (black) as initialized from the parameterized result of the TtoST process (red). Due to the lack of boundary conditions imposed on Γ, TopO was not able to properly account for the formation of boundary layers. ShpO expands to compensate for this.

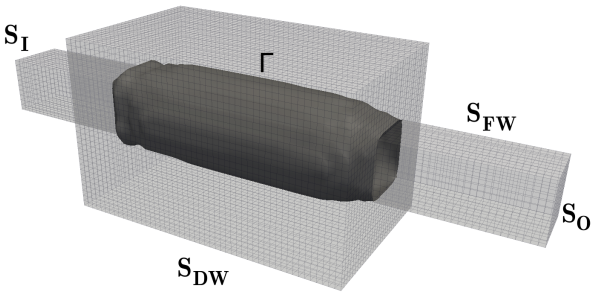

Figure 4: The TopO minimal volume-averaged total pressure loss ϕ solution and geometry of the 3D straight channel case. Entrance channels are 0.5x0.2x0.2m and the design domain is 1.0x0.6x0.6m.

fitting, mesh generation and subsequent shape optimization) will be presented and discussed.

Acknowledgment

This research was funded by the People Programme (ITN Marie Curie Actions) of the European Union's H2020 Framework Programme (MSCA-ITN-2014-ETN) under REA Grant Agreement no. 642959 (IODA project). The first author is an IODA Early Stage Researcher.

References

[1] T. Borvall and J. Peterson, Topology optimization of fluids in Stokes flow. *International Journal for Numerical Methods in Fluids*, **41**, 77-107, 2003.

[2] J.K. Guest and J.H. Prevost, Topology optimization of creeping fluid flows using a Darcy-Stokes finite element. *International Journal for Numerical Methods in Engineering*, **66**, 461-484, 2006.

[3] A. Gersborg-Hansen, O. Sigmund and R. Haber Topology optimization of channel flow problems. *Structural and Multidisciplinary Optimization*, **30**, 181-192, 2005.

[4] O. Pironneau, *Optimal shape design for elliptic systems*. Springer-Verlag, 1984.

[5] D.I. Papadimitriou and K.C. Giannakoglou, Aerodynamic shape optimization using first and second order adjoint and direct approaches. *Archives of Computational Methods in Engineering*, **15**, 447-488, 2008.

[6] E.M. Papoutsis-Kiachagias and K.C. Giannakoglou, Continuous Adjoint Methods for Turbulent Flows, Applied to Shape and Topology Optimization: Industrial Applications. *Archives of Computational Methods in Engineering*, **23-2**, 255-299, 2016.

[7] S. Osher and J.A. Sethian, Fronts Propagating with Curvature Dependent Speed: Algorithms based on Hamilton-Jacobi Formulations. *Journal of Computational Physics*, **79**, 12-49, 1988.

[8] *http://www.openfoam.com*

[9] J. Nocedal and S.J. Wright, *Numerical Optimization*. Springer, 1999.

[10] E.A. Kontoleontos, E.M. Papoutsis-Kiachagias, A.S. Zymaris, D.I. Papadimitriou and K.C. Giannakoglou, Adjoint–based constrained topology optimization for viscous flows, including heat transfer. *Engineering Optimization*, **45**, 941-961, 2013.

[11] J.R.L.Koch, E.M. Papoutsis-Kiachagias and K.C. Giannakoglou, Transition from 2D Continuous Adjoint Level Set Topology to Shape Optimization.

VII European Congress on Computational Methods in Applied Sciences and Engineering, Crete Island, Greece, 5–10 June 2016

[12] J.R.L.Koch, E.M. Papoutsis-Kiachagias and K.C. Giannakoglou, Transition from Adjoint Level Set Topology to Shape Optimization for 2D Fluid Mechanics. *Computers and Fluids*, **10.1016/j.compfluid.2017.04.001**, 2017.

[13] S. Osher and R. Fedkiw, *Level Set Methods and Dynamic Implicit Surfaces*. Springer, 2003.

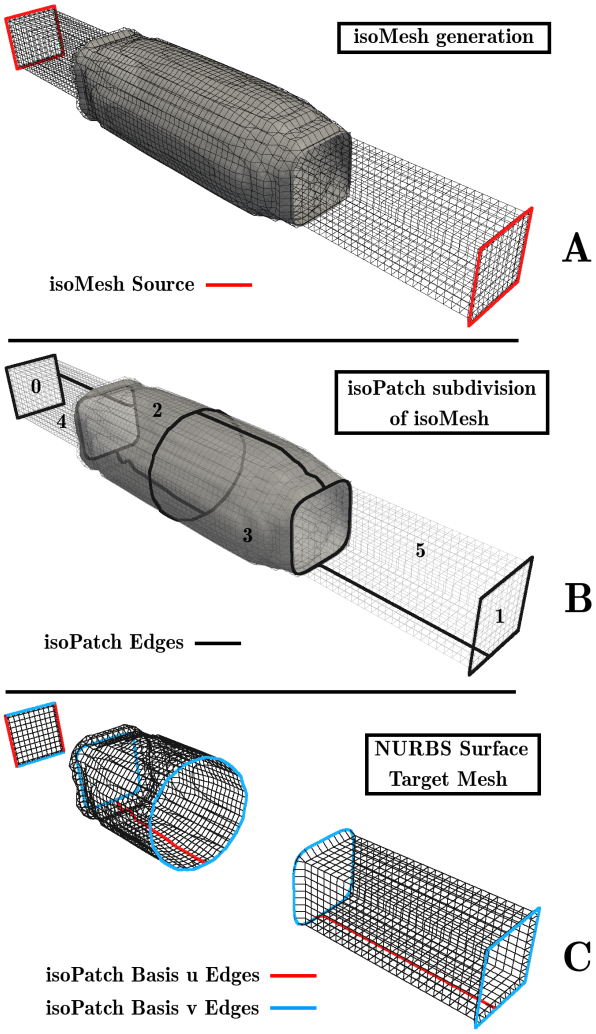

Figure 5: The 3D TtoST process' procedure for subdividing the straight channel's Γ: (A): isoMesh generation. The outer edges of the S_I and S_O case patches act as the mesh generation starting points and are marked in red. (B): isoMesh subdivision. The algorithm generates isoPatches in the order indicated by number, with splitting connections generated automatically as needed. The resulting set of isoPatches is air-tight and represents the entire inlet-outlet connection. (C): isoPatch parameterization. The edges of each isoPatch are ordered to represent the u and v basis of the NURBS surface to fit it. Only isoPatches 0, 2 and 5 are shown for clarity.